JOURNAL OF MASS SPECTROMETRY
J. Mass Spectrom. 2004; **39**: 1450–1455
Published online in Wiley InterScience (www.interscience.wiley.com). DOI: 10.1002/jms.729

JMS

Tandem mass spectrometric data–FAAH inhibitory activity relationships of some carbamic acid O-aryl esters†

Elisa Basso,[1] Andrea Duranti,[2] Marco Mor,[3] Daniele Piomelli,[4] Andrea Tontini,[2] Giorgio Tarzia[2] and Pietro Traldi[1]*

[1] CNR, Istituto di Scienze e Tecnologie Molecolari, Corso Stati Uniti 4, 35127 Padova, Italy
[2] Istituto di Chimica Farmaceutica e Tossicologica, Università degli Studi di Urbino 'Carlo Bo', Piazza del Rinascimento 6, 61029 Urbino (PU), Italy
[3] Dipartimento Farmaceutico, Università degli Studi di Parma, Parco Area delle Scienze 27/A, 43100 Parma, Italy
[4] Department of Pharmacology, University of California, Irvine, 360 MSRII, Irvine, California 92697-4625, USA

Received 8 June 2004; Accepted 13 August 2004

We have recently described a class of systemically active inhibitors of the intracellular activity of fatty acid amide hydrolase (FAAH) and traced extensive structure–activity relationships. These compounds, characterized by an *N*-alkyl carbamic acid *O*-aryl ester structure, exert potent anxiolytic-like effects in animal models. In the present study, possible relationships between mass spectrometric parameters (related to the propensity of the C(O)—O bond to be cleaved) and FAAH-inhibitory potency were tested. With this aim, a set of our products was analyzed by electrospray ionization mass spectrometry and the protonated molecules were decomposed by low-energy collisions. The experiments were performed by ion trap mass spectrometry, which led to a step-by-step energy deposition, thus favouring the lowest critical energy decomposition channels. For all compounds, breakdown curves relative to $[MH]^+$ ions and to the fragment implying C(O)—O bond cleavage were obtained. The crossing point between these curves was related to the energetics of decomposition and the values found for the investigated compounds were linearly correlated ($r^2 = 0.797$) with their FAAH-inhibitory activity. This indicates that the energetics of the C(O)—O bond cleavage may be relevant in explaining FAAH inhibition.

KEYWORDS: carbamates; tandem mass spectrometry; FAAH inhibitory activity; fatty acid amide hydrolase

INTRODUCTION

Various lipid-like substances able to activate cannabinoid (CB) receptors have been discovered in the last decade. Arachidonic acid ethanolamide (anandamide, AEA, **1**, Fig. 1), the first among these endogenous cannabinoids to be discovered,[1] is still the most extensively studied compound of the class. From a neurophysiological point of view, AEA functions as a retrograde synaptic messenger, which, after being released by postsynaptic neurons, diffuses along the synaptic cleft and activates CB_1 receptors on presynaptic nerve terminals, thus inhibiting further liberation of neurotransmitters. AEA action then ceases within a few minutes, because it is reuptaken into the cell by a selective mechanism and degraded there by a serine enzyme, fatty acid amide hydrolase (FAAH).[2] Substances which can block FAAH are considered of therapeutic interest, because, on inhibiting AEA catabolism, they may *inter alia* produce analgesic or anxiolytic actions without the undesired effects that accompany the indiscriminate activation of the system caused by exocannabinoids.

In recent work, we described a class of low molecular mass FAAH inhibitors.[3] These compounds have an *N*-alkyl carbamic acid *O*-aryl ester structure (**2**, Fig. 1) and are systemically active in rats and mice.[4,5] They exert profound anxiolytic-like effects in animal models, which are accompanied by rises in cerebral AEA levels and are blocked by CB_1 receptor antagonists.[4]

Evidence indicates that our carbamate inhibitors of FAAH probably act through an irreversible mechanism.[4] It is reasonable to hypothesize that, like AChE carbamate inhibitors of cholinesterases, compounds **2a–i** (Table 1) may undergo an addition–elimination reaction, ultimately leading to carbamoylation–inactivation of the enzyme. The nucleophile in this reaction is assumed to be Ser241, an amino acid the hydroxyl group of which is activated by other specific residues, as shown in Scheme 1.[6,7] If this hypothesis is correct, the potency of carbamate inhibitors, expressed as the concentration inhibiting 50% (IC_{50}) of

*Correspondence to: Pietro Traldi, CNR, Istituto di Scienze e Tecnologie Molecolari, Corso Stati Uniti 4, 35127 Padova, Italy.
E-mail: pietro.traldi@adr.pd.cnr.it
†Paper presented at the 22nd Informal Meeting on Mass Spectrometry, Tokaj, Hungary, 2–6 May 2004.
Contract/grant sponsor: Ministero dell'Istruzione, dell'Università e della Ricerca (MIUR).
Contract/grant sponsor: University of Parma.
Contract/grant sponsor: University of Urbino.
Contract/grant sponsor: National Institute of Drug Abuse.

Table 1. Inhibitory potency (IC_{50}) values with standard error of the mean (SEM), molecular mass and ESI spectra of compounds **2a–i** (the $[ROH_2]^+$ fragments are generated inside the ESI source)

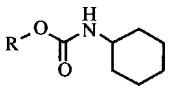

Compound	R	IC_{50} (nM) ± SEM	MW (Da)	ESI spectra: *m/z* (abundance, %)			
				$[M_2 + Na]^+$	$[M + Na]^+$	$[MH]^+$	$[ROH_2]^+$
2a		3776 ± 69	219	461 (100)	242 (70)	220 (35)	
2b		808 ± 42	233	489 (100)	256 (55)	234 (20)	
2c	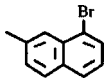	174 ± 31	347	717 (25)	370 (85)	348 (15)	223 (10)
2d	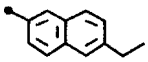	3532 ± 505	297	617 (100)	320 (30)	298 (17)	
2e	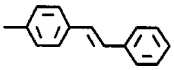	3337 ± 339	321	665 (30)	344 (55)	322 (85)	197 (100)
2f		266 ± 89	321	665 (10)	344 (40)	322 (100)	197 (35)
2g	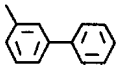	63 ± 9	295	613 (8)	318 (25)	296 (100)	171 (70)
2h	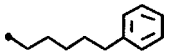	>30 000	289	601 (7)	312 (100)	290 (40)	
2i	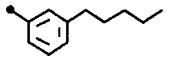	188 ± 36	289	601 (35)	312 (100)	290 (50)	165 (5)

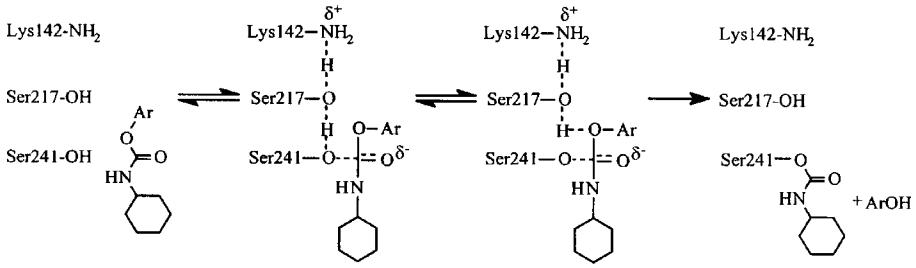

Scheme 1

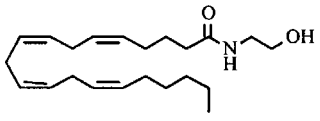

1

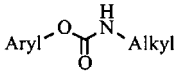

2

Figure 1. Structural formulae of (**1**) arachidonic acid ethanolamide (anandamide, AEA) and (**2**) *N*-alkyl carbamic acid *O*-aryl esters.

tritiated AEA hydrolysis in rat cortical membranes, would be driven by two distinct and sequential molecular processes: (a) the binding of the inhibitors to the enzyme through non-bonded interactions (hydrogen bonds, electrostatic, van der Waals and hydrophobic forces), which is affected by the degree of complementarity between the inhibitor and the active site; and (b) the thermodynamics and kinetics of the carbamoylation reaction (see Scheme 1). The latter is likely to be influenced by the chemical nature of the substituent on the oxygen, since the more stable the leaving group, the greater is the free energy difference between the products of the reaction and the tetrahedral intermediate shown in Scheme 1. (The structure of the aryl substituents might in principle influence the rate of the first stage of the hydrolytic reaction also by modulating the charge density on the carbonyl carbon via an inductive effect. This can be ruled out, however, by noting that the carbonyl carbon ^{13}C NMR chemical shifts of compounds **2a–g,i** fall within a very small range (153.5–153.9 ppm).

The best inhibitory activity in our series of carbamates is observed when the group on the nitrogen is cyclohexyl and that on the oxygen is aromatic, with well-defined spatial characteristics. Our hypothesis that these structures mimic the initial segment of AEA (**1**) in the conformation, referred to as *U-shaped*, was confirmed by the observation that

the more active molecules were those with a bent shape [cf. the IC_{50} of **2g** (63 ± 9 nM, Table 1) and biphenyl-4-yl isomer (2297 ± 226 nM)].[3] A similar difference in activity exists between **2e** and **2f**, **2c** and **2d** and **2b** and its *p*-tolyl isomer.[3] The importance of a curved arrangement of the active molecules is supported by recent docking studies that showed how the *O*-biphenyl-3-yl moiety, and more generally bent-shaped *O*-substituted carbamates, can, in fact, be accommodated in a hydrophobic region of the active site of FAAH, where they counterfeit the segment made up by the first 10–12 carbons of the AEA fatty acid chain.[3]

The above considerations are mainly related to the recognition step of the enzymatic process. Therefore, in order to investigate the catalytic component of FAAH inactivation, we thought it of interest to resort to mass spectrometric (MS) techniques. We considered it useful to estimate the propensity to cleavage of the C(O)—O bond and see whether it could be correlated with the FAAH-inhibitory potency of our compounds. In fact, the shape and electronic nature of the *O*-substituents will affect both the steric and electronic complementarity with the enzyme binding site and the C—O bond dissociation energy; if the latter component is relevant for inhibitory potency, some correlation between the two properties should be observed, even if a certain scattering of the data is to be expected due to the steric effects of the *O*-substituents on the binding component of the catalytic process.

It should be emphasized that interesting results on structure–activity relationships (SAR) by means of mass spectrometric measurements have already been described in the literature.[8–10]

The electrospray ionization (ESI)-induced decomposition and the collisionally induced fragmentation process of the FAAH inhibitors **2a–i** could be regarded as a simplified model of the reaction that these compounds undergo in the biological environment under FAAH catalytic action (see Scheme 1). In particular, ESI and MS/MS experiments may provide information on the behaviour of **2a–i** either in solution or in the gas phase. Protonation processes (and also possible cationization reactions with alkali metals) could take place in solution, before or immediately after the formation of the multi-charged droplets. The protonated molecules might decompose if the compounds exhibit sufficient instability in acidic media. Furthermore, since the ESI source can be approximated to an electrochemical cell, some ionic species could also be produced by redox phenomena occurring in the ionization chamber. The intrinsic behaviour of the protonated molecules, from a thermodynamic point of view, can be validly studied by collisional experiments performed by ion trap. By this approach, the internal energy deposition that takes place during the collisional experiments is a step-by-step phenomenon and consequently the activation of the decomposition channels at the lowest critical energy level are privileged.

EXPERIMENTAL

The syntheses of and pharmacological tests on compounds **2a–i** were as described previously.[3]

Methanol was purchased from Sigma Aldrich (Milan, Italy).

ESI experiments were performed using a LCQ Deca instrument (Thermofinnigan, San Jose, CA, USA) operating in the positive ion mode. Compounds **2a–i** were solubilized in CH_3OH and 10^{-6} M solutions of these compounds were directly infused into the ESI source. The ions were produced using spray voltage, capillary voltage and entrance capillary temperature of 4 kV, 8 V and 220 °C, respectively.

MS/MS experiments were performed by resonant excitation of the ions of interest through a supplementary r.f. voltage in the range 15–40% of its maximum value (5 V peak-to-peak) for 200 ms. The He pressure inside the trap was kept constant: the pressure directly read by ion gauge (in absence of the N_2 stream) was 2.8×10^{-5} Torr (1 Torr = 133.3 Pa). The isolation width was set at 2 mass units. The scan rate was 0.5 s^{-1}.

RESULTS AND DISCUSSION

The ESI spectra of compounds **2a–i** are reported in Table 1. As can be seen, they are particularly simple, yet some specific aspects are worthy of discussion. Protonated molecules are detected for all compounds but, in most cases, their abundance is lower than that of the $[M + Na]^+$ ions, highlighting the affinity of the compounds under investigation for alkali metal ions. This can be explained by the presence of the C(O)O and C(O)N groups, which can readily coordinate Na^+ ions. However, for all the compounds $[M_2 + Na]^+$ ions are also present and their high abundance suggests the pre-existence of these species in the original solutions.

Only in some cases (compounds **2c**,**e–g**,**i**) is the fragment corresponding to the cleavage of the C(O)—O bond detectable in the ESI spectra. It is interesting that these ions do not originate from simple bond cleavage, but require that protonation takes place on the ester oxygen atom and that a further hydrogen rearrangement is needed, reasonably

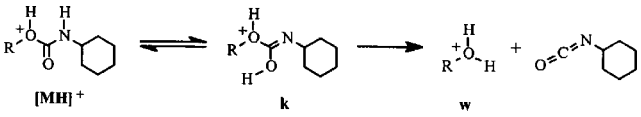

Scheme 2

Table 2. Abundance ratio of the **w** fragment and $[MH]^+$ species present in the ESI spectra of compounds **2a–i** and related pIC_{50} values

Compound	[**w**]/$[MH]^+$	pIC_{50}
2a	0.00	5.42
2b	0.00	6.09
2c	0.67	6.76
2d	0.00	5.45
2e	1.17	5.48
2f	0.35	6.58
2g	0.70	7.20
2h	0.00	Not expressed
2i	0.10	6.73

through the mechanism reported in Scheme 2. The ESI-induced protonation activates a keto-imidic tautomerism leading to species **k** in Scheme 2, which decompose to two thermodynamically highly stable fragments, i.e. neutral cyclohexyl isocyanate and the protonated species **w**. The data reported in Table 2 show that, apart from **2e**, the compounds with lower pIC_{50} values do not lead to the formation of ion **w**. The anomalous behaviour of **2e** might be explained by assuming that non-covalent interactions occurring in the recognition step of the catalytic process predominate over the C(O)—O cleavage in determining pIC_{50}.

The reaction leading to the fragment **w** detected in the ESI spectra may originate through a mechanism occurring in solution (either because of the acidic conditions originating inside the multi-charged droplets or of redox events taking place inside the ESI source[11]) or by 'in-source' collisional phenomena. Considering that the capillary voltage was maintained at a constant, low level (8 V), it is reasonable to assume that the former mechanism is the most effective one. To verify whether these processes may serve as a model of the reactivity of these compounds in a biological environment, roughly expressed as a pIC_{50} value, the abundance ratio $[\mathbf{w}]/[MH]^+$ for the compounds under study was determined. Such a parameter may be indicative of the ease of C(O)—O cleavage. We observed, however, that the $[\mathbf{w}]/[MH]^+$ values are not statistically correlated with the pIC_{50} values.

To pursue a more reliable correlation, the compounds were further investigated by collisional experiments performed on protonated molecules. As an example, the MS (top) and MS/MS (bottom) spectra of compound **2g** are reported in Fig. 2. In this case the data obtained are of a purely thermodynamic nature. In other words, the decomposition pathway and the yield of decomposition products depend only on the related critical energies, and consequently by the energy deposition on $[MH]^+$ achieved by collision. In this regard, ion trap technology is highly effective: in fact, whereas high- and low-energy collisions performed by sector instruments, or a triple quadrupole device, lead to a rather wide internal energy distribution (owing to the statistics of the collisional phenomena), an ion trap operating in ion resonance mode leads to a step-by-step internal energy deposition, favouring the decomposition processes at low critical energy. Furthermore, by varying the supplementary r.f. voltage, responsible for the collisional activation, it is possible to obtain well reproducible plots of the variation of the precursor ion and fragment ion abundances versus collisional energy. These plots, usually called breakdown curves, effectively highlight differences in decomposition energy of pre-selected species. In particular, considering the crossing point (CP) between the plots of precursor ion abundance and fragment ion abundance, it is possible to obtain a parameter (corresponding to the collision energy necessary to fragment 50% of the precursor ion population) closely related to the critical energy of the decomposition processes. As an example, the breakdown curves obtained for compounds **2c** and **2e** are reported in Fig. 3. Thus, for **2c** the CP value is at 0.94 ± 0.02 V whereas for **2e** it is at 1.11 ± 0.02 V, indicating that, for **2c**, the decomposition process (from $[MH]^+$ to **w**) related to the C(O)—O bond cleavage with H rearrangement is energetically more favourable than in the case of **2e**.

The CP values for the compounds under study, representing the mean values of five determinations, and the related standard deviations, are reported in Table 3. It is noteworthy that under collisional conditions **2h**, which exhibits the lowest pIC_{50} value, does not lead to the fragment related to the C(O)—O bond cleavage. Moreover, significant differences were obtained for the compounds of the series. We plotted pIC_{50} against CP values (Fig. 4) and derived the following

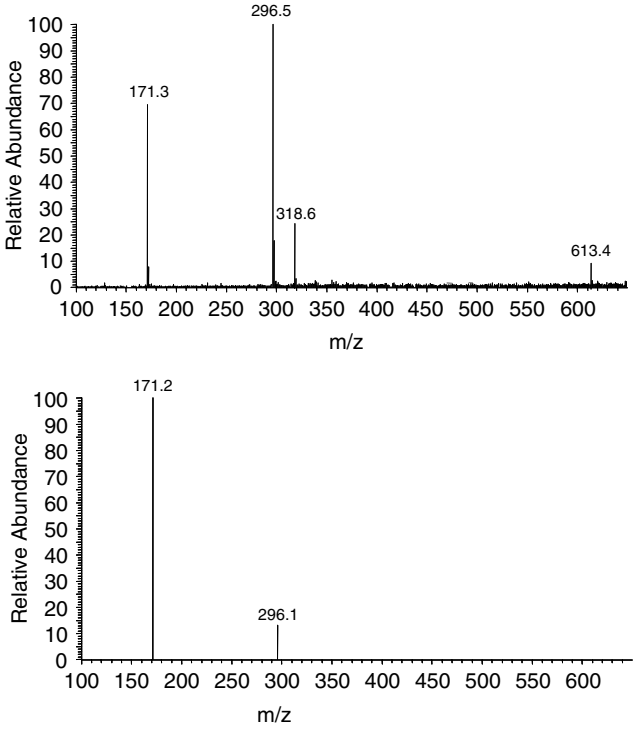

Figure 2. MS (top) and MS/MS (bottom) spectra of **2g**.

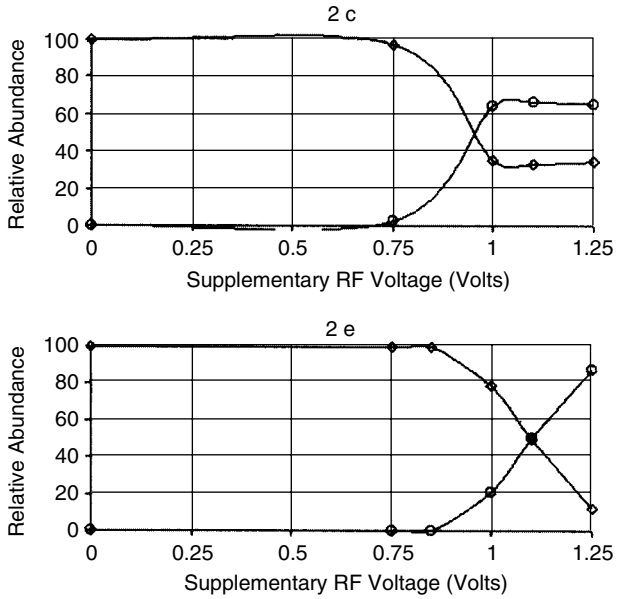

Figure 3. Breakdown curves obtained by collision of ESI-generated $[MH]^+$ species of **2c** (top) and **2e** (bottom). The relative abundances of $[MH]^+$ (◊) and $[ROH_2]^+$ fragments (○) (see Scheme 2) are plotted with respect to the supplementary r.f. voltage.

Table 3. Values of the crossing points determined in the breakdown curves obtained by collision of $[MH]^+$ species of compounds **2a–i** and related pIC_{50} values

Compound	Crossing point (V)	pIC_{50}
2a	1.10 ± 0.02	5.42
2b	0.98 ± 0.05	6.09
2c	0.94 ± 0.02	6.76
2d	1.09 ± 0.08	5.45
2e	1.11 ± 0.02	5.48
2f	1.03 ± 0.04	6.58
2g	0.96 ± 0.03	7.20
2h	Not expressed	Not expressed
2i	0.96 ± 0.04	6.73

equation:

$$pIC_{50} = -8.886\ (\pm 1.834)CP + 15.289(\pm 1.876)$$
$$n = 8; R^2 = 0.797; s = 0.342; F = 23.5$$

CP can therefore explain almost 80% of pIC_{50} variation; the standard error is not too large, in comparison with those commonly encountered in quantitative SAR (QSAR);[12] therefore, part of the inhibitory potency variation may be attributed to effects involved in the binding component of the catalytic process. From Fig. 4, it can be observed that **2g** and **2f**, which were more potent than expected from their CP, are characterized by a bent shape which, in a 3D-QSAR model[3] that we have reported previously, was positively correlated with FAAH inhibitor potency.

This correlation suggests that the thermodynamics of the hydrolytic reaction may play a role in the potency of these carbamates and offers some indication about their mechanism of action. The three-dimensional model in Fig. 5 supports the idea that, in accord with the mechanism in Scheme 1, after the nucleophilic attack of Ser241 on the carbonyl and a proton shift also involving Ser217 and Lys142, the side-chain of Ser217 is sufficiently close to the phenolic oxygen to participate in its protonation. However, an alternative orientation of the inhibitor is possible, which allows the superposition of the biphenyl scaffold on the arachidonyl chain of MAP and which gives

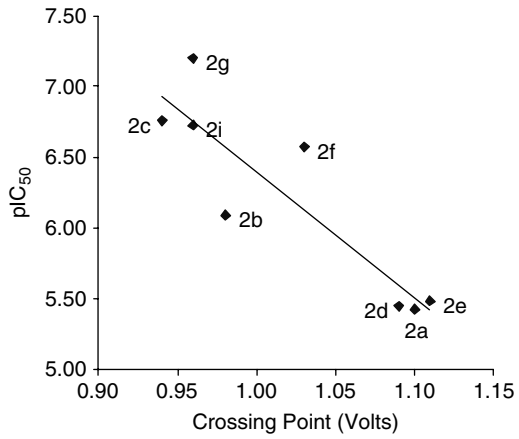

Figure 4. Plot of pIC_{50} vs crossing point values obtained by the breakdown curves related to $[MH]^+$ species.

better stereoelectronic complementarity with the enzyme binding cavity.[14] A detailed comparison between the two docking solutions[14] is under investigation.

The correlation presented here between the energy of C(O)—O bond cleavage and IC_{50} values supports the mechanism in Scheme 1. Furthermore, it provides some evidence that a mechanism via extrusion of cyclohexylamine, analogous to that by which AEA is hydrolysed by FAAH,[7] is not operative in the FAAH-mediated hydrolysis of *N*-alkyl-*O*-aryl carbamates. On the contrary, the present data, obtained under conditions favouring ESI-induced protonation of the molecules under study, cannot be used to decide whether the mechanism operating in the alkaline hydrolysis of *N*-monosubstituted aryl carbamates contributes to the hydrolysis of the carbamates. This implies removal of the proton from the nitrogen atom, formation of an isocyanate by elimination of ArO^- and eventually decomposition of this isocyanate into CO_2 and RNH_2 by water.[15] Such a process, however, could be reasonably excluded since it would imply the presence of a residue in the vicinity of the NH group, basic enough to deprotonate it. An inspection of the x-ray model of the active site demonstrates that no such residue actually exists.

In conclusion, the present results, obtained by ESI-induced protonation of the molecules under study and their collisionally induced decompositions of $[MH]^+$ species, highlight a correlation between the lability of the carbamate C(O)—O bond and inhibitory potency. Hence the ability

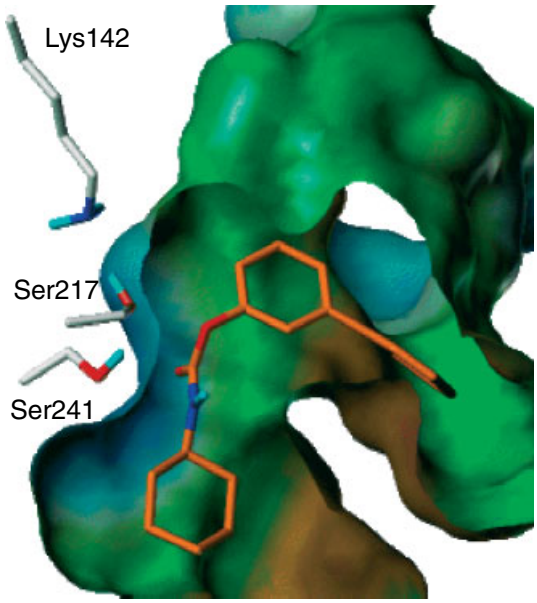

Figure 5. Docking of **2g** within the FAAH catalytic site, built from the coordinates of the enzyme covalently bound to methyl arachidonyl phosphonate (MAP).[13] MAP coordinates were removed and hydrogen atoms added (only the polar ones are shown). A molecular model of **2g** was docked into the enzyme cavity selecting an orientation which allowed a short distance between the phenolic oxygen of **2g** and the oxygen of Ser217. Energy minimization by MMFF94s force field implemented in Sybyl 6.9 (Tripos, St. Louis, MO, USA) gave the structure illustrated, having a 2.83 Å distance between the two oxygen atoms.

of the phenolic fragment to act as a leaving group after the nucleophilic attack of the active serine seems to be relevant for enzyme covalent inhibition. The importance of the carbamate protonation during the inhibition steps and its relative orientation within the catalytic site are crucial points to elucidate the mechanism of action of the present compounds and deserve further investigation. These mechanistic issues will be better addressed in future studies.

Acknowledgements

This work was supported by MIUR (Ministero dell'Istruzione, dell'Università e della Ricerca), the Universities of Parma and Urbino and the National Institute of Drug Abuse (to D.P.). The CCE (Centro di Calcolo Elettronico) and CIM (Centro Interfacoltà Misure) of the University of Parma are gratefully acknowledged for supplying the Sybyl software license. Thanks are due to Dr Giuseppe Gatti for discussing ^{13}C NMR spectra.

REFERENCES

1. Devane WA, Hanuš L, Breuer A, Pertwee RG, Stevenson LA, Griffin G, Gibson D, Mandelbaum A, Etinger A, Mechoulam R. Isolation and structure of a brain constituent that binds to the cannabinoid receptor. *Science* 1992; **258**: 1946.
2. Piomelli D. The molecular logic of the cannabinoid signalling. *Nat. Rev. Neurosci.* 2003; **4**: 873.
3. Tarzia G, Duranti A, Tontini A, Piersanti G, Mor M, Rivara S, Plazzi PV, Park C, Kathuria S, Piomelli D. Design, synthesis, and structure–activity relationships of alkylcarbamic acid aryl esters, a new class of fatty acid amide hydrolase inhibitors. *J. Med. Chem.* 2003; **46**: 2352.
4. Kathuria S, Gaetani S, Fegley D, Valiño F, Duranti A, Tontini A, Mor M, Tarzia G, La Rana G, Calignano A, Giustino A, Tattoli M, Palmery M, Cuomo V, Piomelli D. Modulation of anxiety through blockade of anandamide hydrolysis. *Nat. Med.* 2003; **9**: 76.
5. Piomelli D, Duranti A, Tarzia G, Tontini A, Mor M. Modulation of anxiety through blockade of anandamide hydrolysis. PCT Int. Appl. 033 422, 2004.
6. Patricelli MP, Lovato MA, Cravatt BF. Chemical and mutagenic investigations of fatty acid amide hydrolase: evidence for a family of serine hydrolases with distinct catalytic properties. *Biochemistry* 1999; **38**: 9804.
7. McKinney MK, Cravatt BF. Evidence for distinct roles in catalysis for residues of the serine–serine–lysine catalytic triad. *J. Biol. Chem.* 2003; **278**: 37 393.
8. Orsatti L, Seraglia R, Traldi P, Diamantini G, Tarzia G, Tontini A. Electron ionization and fast atom bombardment mass spectrometry of some 3,3-dimethyl-1-(isoxazol-3-yl)triazenes. A new class of potential anticancer agents. *J. Mass Spectrom.* 1995; **30**: 1567.
9. Tarzia G, Diamantini G, Tontini A, Favretto D, Traldi P. Correlation of the mutagenic properties of aryl- and heteroaryltriazenes with their electron ionization induced fragmentation. *Rapid Commun. Mass Spectrom.* 1996; **10**: 1156.
10. Tarzia G, Diamantini G, Tontini A, Bedini A, Favretto D, Traldi P. Correlation of the antimetastatic properties of aryltriazenes with their electron impact ionization mass spectra. *Rapid Commun. Mass Spectrom.* 1997; **11**: 1365.
11. De la Mora JF, Van Berkel GJ, Enke CG, Cole RB, Martinez-Sanchez M, Fenn JB. Electrochemical processes in electrospray ionization mass spectrometry. *J. Mass Spectrom.* 2000; **35**: 939.
12. Hansch C, Leo A. *Exploring QSAR. Fundamentals and Applications in Chemistry and Biology*. American Chemical Society: Washington, DC, 1995; 535.
13. Bracey MH, Hanson MA, Masuda KR, Stevens RC, Cravatt BF. Structural adaptation in a membrane enzyme that terminates endocannabinoid signaling. *Science* 2002; **298**: 1793.
14. Mor M, Rivara S, Lodola A, Plazzi PV, Tarzia G, Duranti A, Tontini A, Piersanti G, Kathuria S, Piomelli D. Cyclohexylcarbamic acid 3′- or 4′-substituted biphenyl-3-yl esters as fatty acid amide hydrolase inhibitors: synthesis, quantitative structure–activity relationships and molecular modelling studies. *J. Med. Chem.* 2004; in press.
15. Smith MB, March J. In *March's Advanced Organic Chemistry—Reactions, Mechanism and Structure*. J Wiley: New York, 2001; 474, and references cited therein.